

Accepted Manuscript

Discovery of simplified sampangine derivatives as novel fungal biofilm inhibitors

Na Liu, Hua Zhong, Jie Tu, Zhigan Jiang, Yanjuan Jiang, Yan Jiang, Yuanyin Jiang, Jian Li, Wannian Zhang, Yan Wang, Chunquan Sheng



PII: S0223-5234(17)30843-7

DOI: [10.1016/j.ejmech.2017.10.043](https://doi.org/10.1016/j.ejmech.2017.10.043)

Reference: EJMECH 9835

To appear in: *European Journal of Medicinal Chemistry*

Received Date: 23 July 2017

Revised Date: 28 September 2017

Accepted Date: 15 October 2017

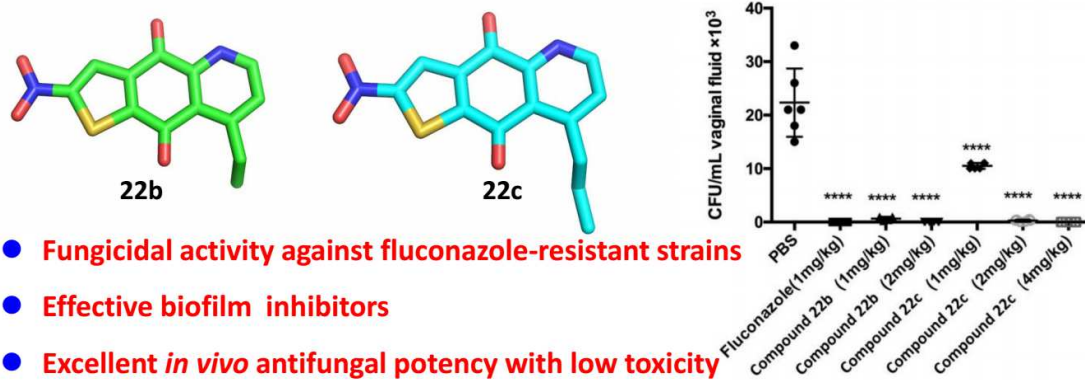
Please cite this article as: N. Liu, H. Zhong, J. Tu, Z. Jiang, Y. Jiang, Y. Jiang, Y. Jiang, J. Li, W. Zhang, Y. Wang, C. Sheng, Discovery of simplified sampangine derivatives as novel fungal biofilm inhibitors, *European Journal of Medicinal Chemistry* (2017), doi: 10.1016/j.ejmech.2017.10.043.

This is a PDF file of an unedited manuscript that has been accepted for publication. As a service to our customers we are providing this early version of the manuscript. The manuscript will undergo copyediting, typesetting, and review of the resulting proof before it is published in its final form. Please note that during the production process errors may be discovered which could affect the content, and all legal disclaimers that apply to the journal pertain.

Graphical Abstract

Discovery of Simplified Sampangine Derivatives as Novel Fungal Biofilm Inhibitors

Na Liu^{1,#}, Hua Zhong^{1,#}, Jie Tu^{1,#}, Zhigan Jiang¹, Yanjuan Jiang¹, Yan Jiang¹, Yuanyin Jiang¹, Jian Li², Wannian Zhang^{1,*}, Yan Wang^{1,*}, Chunquan Sheng^{1,*}



Novel simplified analogues of natural product sampangine showed excellent *in vitro* and *in vivo* antifungal activity with promising features to overcome fluconazole-related and biofilm-related drug resistance.

Discovery of Simplified Sampangine Derivatives as Novel Fungal Biofilm Inhibitors

Na Liu^{1,#}, Hua Zhong^{1,#}, Jie Tu^{1,#}, Zhigan Jiang¹, Yanjuan Jiang¹, Yan Jiang¹, Yuanyin Jiang¹, Jian Li², Wannian Zhang^{1,*}, Yan Wang^{1,*}, Chunquan Sheng^{1,*}

¹ School of Pharmacy, Second Military Medical University, 325 Guohe Road, Shanghai 200433, People's Republic of China

² School of Pharmacy, East China University of Science & Technology, 130 Meilong Road, Shanghai 200237, People's Republic of China

[#]These two authors contributed equally to this work.

* To whom correspondence should be addressed. For C. Q. Sheng: Phone/Fax, 86-21-81871239, E-mail, shengcq@smmu.edu.cn; For Y. Wang: Phone/Fax, 86-21-81871260, E-mail, wangyansmmu@126.com; For W.N. Zhang: Phone/Fax, 86-21-81871243, E-mail, zhangwnk@hotmail.com.

Abstract: Lack of novel antifungal agents and severe drug resistance have led to high incidence and associated mortality of invasive fungal infections. To tackle the challenges, novel antifungal agents with new chemotype, fungicidal activity and anti-resistant potency are highly desirable. On the basis of our previously identified simplified analogue of antifungal natural product sampangine, systemic structure-activity relationships were clarified and two novel derivatives showed promising features as novel antifungal lead compounds. Compounds **22b** and **22c** showed good fungicidal activity against both fluconazole-sensitive and fluconazole-resistant *Candida albicans* strains. Moreover, they were proven to be potent inhibitors of *Candida albicans* biofilm formation and yeast-to-hypha morphological transition by down-regulating biofilm-associated genes. In a rat vaginal *Candida albicans* infection model, compounds **22b** and **22c** showed excellent therapeutic effects with low toxicity. The results highlighted the potential of sampangine derivatives to overcome fluconazole-related and biofilm-related drug resistance.

Keywords: Sampangine, antifungal activity, biofilm inhibition, anti-resistance

1. Introduction

Life-threatening invasive fungal infections (IFIs) are regarded as the “hidden killers” of immunocompromised individuals such as patients with AIDS, cancer and organ transplantation [1]. Recently, IFIs are associated with high incidence and high mortality and become a serious health problem in clinic [2]. IFIs are predominantly caused by Candidiasis (*Candida albicans*, mortality: 46% - 75%), cryptococcosis (*Cryptococcus neoformans*, mortality: 20% - 70%), and aspergillosis (*Aspergillus fumigates*, mortality: 30% - 95%) [1]. Despite the high mortality of IFIs, effective and safe antifungal agents are rather limited [3]. Clinically, antifungal agents for the treatment of IFIs mainly include azoles (*e.g.* fluconazole, voriconazole, itraconazole, posaconazole and isavuconazole), polyenes (*e.g.* amphotericin B) and echinocandins (*e.g.* caspofungin and micafungin) [4]. However, these antifungal drugs have only achieved modest success in reducing the high mortality rates of IFIs [5]. Therapeutic limitations of current antifungal agents mainly consist of low efficacy, narrow spectrum, significant toxicity, drug-drug interactions and unfavorable pharmacodynamic (PD) and pharmacokinetic (PK) profiles [6]. Notably, severe resistance has been observed in almost all of the clinically available antifungal agents [7, 8]. As a result, their therapeutic effects are significantly reduced, which is an important contributing factor to the high mortality. Thus, discovery and development of safer and more effective antifungal drugs is highly desirable and urgently needed.

Currently, only a few antifungal candidate drugs are currently in preclinical or clinical development, most of which are structural analogues of azoles and echinocandins [9]. However, these follow-on drugs with the same mode of action can hardly solve the resistance and toxicity problems. Thus, identification of novel antifungal molecular scaffold is of great importance for discovery of new generation of antifungal agents [10]. Natural products provide a rich and unique source of antifungal lead compounds [11]. For example, polyenes and echinocandins are derived from natural products. However, it also should be noted that these nature products-based antifungal agents are generally limited by synthetic difficulty, undesired PK profiles and poor oral availability due to their complex chemical structures [11]. To tackle the challenges, clarifying structural determinants for antifungal activity and structural simplification of antifungal natural products presents a promising strategy. Nevertheless, it is difficult to identify a simplified scaffold with similar or even better antifungal activity.

Previously, we reported a successful example of structural simplification of antifungal natural product sampangine [12, 13]. As compared with sampangine, simplified analogue **3 (ZG-20-7)** showed better antifungal activity, improved water solubility, low toxicity and promising anti-resistance profiles, which represents a good starting point for the discovery of new generation of antifungal agents [13]. However, detailed structure-activity relationship (SAR) of compound **3** is still unknown. More importantly, its *in vivo* antifungal

potency remains to be further improved. Herein, systemic SAR of lead compound **3** was investigated. Two derivatives, **22b** and **22c**, showed excellent *in vitro* and *in vivo* antifungal activity with promising features to overcome fluconazole-related and biofilm-related drug resistance.

2. Results and Discussion

2.1 Chemistry

Chemical synthesis of the simplified sampangine derivatives is depicted in **Schemes 1–5**. Compounds **3** and **9** were synthesized from 6,7-dihydrobenzo[*b*]thiophen-4(5*H*)-one (**4**) via five steps [13]. Then, the nitro groups were reduced to amine groups in the presence of NaBH₄, NiCl₂ and MeOH/DMF to afford compounds **10a** and **10b** (**Scheme 1**).

Starting from compound **3**, the carbonyl groups were reduced to the hydroxyl groups (**11a** and **11b**) in the presence of NaBH₄ and DMF. Then, the two hydroxyl groups were removed to form the aromatization product **12** under the acid condition. Using hydrogen peroxide as the oxidant, the *N*-oxide derivative **13** was prepared. Bromination of the methyl group of compound **3** by Br₂ in HOAc at 110 °C yielded the di-bromo derivative **14**. After further oxidation in the presence of DMSO, the formyl derivative **15** was obtained, which was reacted with the Wittig reagent to form the α , β -unsaturated esters **16a** and **16b** (**Scheme 2**).

Intermediate **20** was synthesized from 6,7-dihydrobenzo[*b*]thiophen-4(5*H*)-one (**4**) via four steps [13]. Then, it was reacted with different hydrazones (**21a-u**) by the Diels-Alder reaction to form various C7- and C8-substituted analogues (**22a-u**,

Scheme 3).

2.2 SAR of the Simplified Sampangine Derivatives

The SAR of lead compound **3** was focused on the nitro group, thiophene ring, benzoquinone ring, pyridine ring and its substitutions. A number of derivatives were synthesized and assayed, whose antifungal activity was expressed as the minimal inhibitory concentration (MIC) that achieved 80% inhibition of the tested fungal pathogens. First, the importance of the nitro group was investigated. The movement of the nitro group from position 2 to 3 (compound **9**) led to decrease of the antifungal activity. When the nitro group was reduced to amine, compounds **10a** and **10b** were almost inactive. Only compound **10a** showed moderate activity against *T. rubrum* ($MIC_{80} = 8 \mu\text{g/mL}$). Second, the benzoquinone carbonyl groups were reduced to the hydroxyl groups (**11a** and **11b**). Interestingly, the antifungal activity of the *cis* isomer **11b** was slightly decreased (MIC_{80} range: 2 to 16 $\mu\text{g/mL}$), whereas the *trans* isomer **11a** was totally inactive. Further removal of the benzoquinone carbonyl groups also resulted in general loss of the antifungal activity. Compound **12** were only moderately active against *C. glabrata* and *T. rubrum*. Moreover, the benzoquinone containing scaffolds did not possess antifungal activity. As described in **Table 2**, compounds **23-26** [12] were generally inactive against the tested fungal pathogens, indicating that the benzoquinone substructure was not the determinant for the antifungal activity. Intermediate **8** with the thiophene substructure showed moderate antifungal activity and further incorporation of a nitro group led to significant improvement of the antifungal activity (**Table 1**). Thus, the 2-nitrothirno[2,3-g]quinoline-4,9-dione played

key roles for the antifungal activity.

Third, the effects of the pyridine ring and its substitutions were explored. Obvious decrease of the antifungal activity was observed for *N*-oxide derivative **13**. Furthermore, a number of C7- and C8-substituted derivatives were synthesized and assayed. Removal of the C8 methyl group had little effect on the antifungal activity (compound **22f**). In contrast, di-bromo derivative **14** and formyl derivative **15** generally showed decreased activity. Even though, compound **15** was highly active against *C. glabrata* ($\text{MIC}_{80} = 0.125 \mu\text{g/mL}$), which was more potent than lead compound **3**, sampangine, fluconazole and itraconazole. However, further extension of the formyl group by α , β -unsaturated esters (**16a** and **16b**) were unfavorable for the antifungal activity. When the C8-methyl group was extended to ethyl (**22b**), propyl (**22c**) or butyl (**22d**) group, good antifungal activity was retained. Similarly, movement of the C8-methyl group to C7 position was also tolerable and compound **22e** was comparable to lead compound **3**. Replacement of the C7-methyl group by ethyl (**22g**), propyl (**22h**), butyl (**22i**), isopropyl (**22j**) and *tert*-butyl (**22k**) led to slight decrease of the antifungal activity. However, when more bulky groups, such as phenyl groups and heterocycles, were attached on the C7 (**22q-t**) or C8 (**22l-p**) position, antifungal activity was decreased obviously. In addition, compounds **26a-m** with larger C8-amide substitutions were totally inactive. Interestingly, compound **22a** with C7 and C8 dimethyl substitution showed excellent activity against *C. albicans* ($\text{MIC}_{80} = 0.25 \mu\text{g/mL}$), *C. parapsilosis* ($\text{MIC}_{80} = 0.5 \mu\text{g/mL}$), *C. neoformans* ($\text{MIC}_{80} = 0.5 \mu\text{g/mL}$), and *A. fumigatus* ($\text{MIC}_{80} = 1 \mu\text{g/mL}$). Its activity was comparable or

superior to that of flconazole and lead compound **3**.

On the basis of the above analysis, primary SAR can be obtained (**Fig. 2**). For the thiophene substitution, C2-nitro group was important for the antifungal activity. Small alkyl substitution is favored at both C7 and C8 position on the pyridine and the methyl group performed the best. Also, di-methyl substitution on C7 and C8 yielded a highly active compound **22a**. In contrast, bulky groups at C7 or C8 position led significant decrease or loss of the antifungal activity. The hydrogen bond donor seems to be important for the C4 and C9 position and carbonyl group was better than hydroxyl group.

2.3 Compounds **22b** and **22c** Shows Selective and Remarkable Fungicidal Activity Including Fluconazole-resistant Clinical Isolates

Compounds **22a**, **22b**, **22c** and **22e** showed excellent antifungal activity with a broad spectrum, which were subjected for further biological evaluations. According to the results of MIC₈₀ in 24 h listed in **Table 1**, we further evaluated the antifungal activity of compounds **22a-c** and **22e** against *C. albicans* in 48 h. The four candidates showed an MIC₈₀ value of 4 µg/mL, 0.25 µg/mL, 0.5 µg/mL, and 0.5 µg/mL, respectively, which was comparable or superior to fluconazole (MIC₈₀ = 0.5 µg/mL). Because 0.5 µg/mL of compounds **22a** and **22e** couldn't completely inhibited *C. albicans* hyphal growth in the following yeast-to-hypha morphological transition assay (**Fig. S1** in Supporting Information), only compounds **22b** and **22c** were further evaluated.

Due to severe drug resistance of fluconazole, clinically resistant *C. albicans*

strains, such as 032, 1010, J38, 103 and chang7, were used to evaluate the potency of compounds **22b** and **22c** to treat resistant fungal infections (**Table 3**). To our delight, both of them exhibited excellent inhibitory activity against those clinical drug-resistant *C. albicans* with MIC₈₀ values in the range of 0.25 to 1 µg/mL. Moreover, time-kill curve assay was further carried out to evaluate their fungicidal effects. In accordance with the MIC results, both of them exhibited dramatic fungicidal activity. More specifically, 0.8 µg/mL of compounds **22b** or **22c** showed remarkable fungicidal effect on *C. albicans* (**Fig. 3A and B**, $P < 0.001$).

Compounds **22b** and **22c** were assayed for antibacterial and antitumor activity. Both compounds were inactive against two strains of *Staphylococcus aureus* (MIC > 128 µg/mL) and the Capan-1 cancer cell line (IC₅₀ > 100 µM), indicating that they had selective antifungal activity.

2.4 Compounds 22b and 22c Effectively Inhibited *C. albicans* Biofilm Formation

C. albicans biofilms usually lead to drug resistance and repeated infection in clinic [14]. Fluconazole can inhibit biofilm formation for only 60% at the concentration as high as 1024 µg/mL [15], and antifungal agents with anti-biofilm activity are urgently needed [16]. Thus, we further evaluated the anti-biofilm activity of compounds **22b** and **22c**. Interestingly, compounds **22b** and **22c** exhibited remarkable anti-biofilm activity (**Fig. 4A and B**). Compounds **22b** (6.4 µg/mL) or **22c** (12.8 µg/mL) disrupted the formation of *C. albicans* biofilms thoroughly.

Scanning electron microscopy (SEM) assay was conducted to confirm the anti-biofilm activity of compounds **22b** and **22c**. In contrast to the proliferated *C.*

albicans biofilm in the control group, the biofilm structure was apparently disrupted by compounds **22b** and **22c**. 0.8 $\mu\text{g}/\text{mL}$ of compound **22b** or **22c** disrupted the formation of *C. albicans* biofilms thoroughly (**Fig. 5**).

2.5 Compounds 22b and 22c Inhibited Yeast-to-hypha Morphological Transition of *C. albicans*

Adhesion and hyphal formation are both essential for *C. albicans* biofilm formation [14]. Initially, we investigated the inhibition effect of compounds **22a-c** and **22e** on the yeast-to-hypha morphological transition of *C. albicans* (**Fig. S1** in Supporting Information). Compounds **22b** and **22c** both exhibited inhibitory effect at 0.25 $\mu\text{g}/\text{mL}$, and completely inhibited hyphal growth at 0.5 $\mu\text{g}/\text{mL}$, whereas compounds **22a** and **22e** couldn't completely inhibited hyphal growth at the high concentration of 0.5 $\mu\text{g}/\text{mL}$. Since cellular surface hydrophobicity (CSH) can indicate the adhesion ability of *C. albicans* [17-19], we examined the effect of compounds **22b** and **22c** on CSH of *C. albicans*. Both compounds could decrease the CSH of *C. albicans* to some extent (**Fig. 6A** and **6B**). Moreover, we investigated the effect of compounds **22b** and **22c** on hyphal formation of *C. albicans* in different inducing media. Five hypha-inducing media were used, including YPD containing 10% fetal bovine serum (FBS), Lee, Spider, SLAD and RPMI 1640 medium. Among these media, YPD containing FBS is the most potent hypha inducer [20]. In our study, *C. albicans* could form long hyphae as expected in all the media tested. Both compounds **22b** and **22c** inhibited hyphal formation in a dose-dependent manner. 0.4 $\mu\text{g}/\text{mL}$ of compound **22b** or **22c** could inhibit hyphal formation obviously in Lee, Spider, SLAD and RPMI 1640 medium

(**Fig.S2A** and **S2B** in Supporting Information). 1.6 µg/mL of compound **22b** or **22c** disrupted hyphal formation thoroughly, even in the most potent hypha inducer YPD containing FBS (**Fig. 7**).

2.6 Anti-biofilm Mechanism of Compounds 22b and 22c by Real-time RT-PCR

To better understand the anti-biofilm mechanism of compounds **22b** and **22c**, we conducted real-time RT-PCR to investigate the expression of some important biofilm-associated genes (**Fig. 8**) [21-23]. Hypha-specific genes *ECE1* [24], *HGCI* [25], *HWP1* [26], *UME6* [27] were down-regulated after treatment with 0.4 µg/mL of compound **22b** or **22c**. Adhesion-specific genes, *ALS3* [28] and *EAP1* [29], were also down-regulated. Interestingly, some important regulation genes in RAS/MAPK or RAS/cAMP pathways, including *RAS1* [21], *CYR1* [21, 30], *EFG1* [31], *CEK1* [32] and *CPHI* [33] were down-regulated too. Collectively, both **22b** and **22c** could down-regulate biofilm-associated genes.

2.7 Compounds 22b and 22c Shows Potent in vivo Antifungal Activity with Low Toxicity

The *in vivo* anti-fungal activities of compounds **22b** and **22c** were investigated using a rat vaginal infection model. Vulvovaginal candidiasis (VVC) has high incidence (about 75%) in women, which is mainly caused by *C. albicans* [34]. On the basis of the antifungal mechanism of compounds **22b** and **22c**, this model is ideal for evaluating the *in vivo* antifungal potency because VVC infections rely on fungal morphogenesis and biofilm formation [35]. Rats were intravaginally inoculated with *C. albicans* to cause vaginal infection, and then treated with compound **22b**, **22c** or

fluconazole as a control. Both compounds **22b** and **22c** effectively reduced fungal burden after infection. More specifically, at 1 mg/kg, both compounds **22b** and **22c** could significantly alleviate vaginal fungal burden (**Fig. 9A**, $P < 0.0001$), and the effect of compound **22b** was comparable to fluconazole. Moreover, we evaluated the toxicity of compounds **22b** and **22c** using the model organism *Caenorhabditis elegans* (*C. elegans*). Under different concentrations (6.25 to 100 $\mu\text{g mL}^{-1}$), no toxicity was observed (**Fig. 9B**), indicating a promising prospect for clinical applications.

3. Conclusions

The treatment of resistant IFIs remains a challenging task. On the basis of our previously identified thieno[2,3-*g*]quinoline-4,9-dione antifungal scaffold, systemic SARs were clarified and highly potent sampangine derivatives were identified. Compounds **22b** and **22c** showed remarkable antifungal activity both *in vitro* and *in vivo*. Especially, they were fungicidal against fluconazole-resistant *C. albicans* strains and were proven to be potent biofilm inhibitors. The results highlighted the potential of the sampangine derivatives to overcome fluconazole-related and biofilm-related drug resistance. Further structural optimization, antifungal mechanism and therapeutic potential of these simplified sampangine derivatives are in progress.

4. Experimental section

4.1. Chemistry

General Methods. Nuclear magnetic resonance (NMR) spectra were recorded on a Bruker 400 spectrometer at room temperature, with tetramethylsilane (TMS) as an internal standard. Chemical shifts (δ) are reported in parts per million (ppm), and

signals are reported as s (singlet), d (doublet), t (triplet), q (quartet), m (multiplet), or br s (broad singlet). High-resolution mass spectrometry data were collected on a Kratos Concept mass spectrometer. TLC analysis was carried out on silica gel plates GF254 (Qingdao Haiyang Chemical, China). Silica gel column chromatography was performed with Silica gel 60 G (Qingdao Haiyang Chemical, China). Unless otherwise noted, all materials were obtained from commercial suppliers and used without further purification. Chemical purities were analyzed by HPLC using MeOH/H₂O as the mobile phase with a flow rate of 0.6 mL/min on a C18 column. All final compounds exhibited the purity greater than 95%.

Starting from 6,7-dihydrobenzo[*b*]thiophen-4(5*H*)-one (**4**), intermediates **8** and **20** were prepared via four steps according to our previously reported methods [12, 13].

4.1.1. 8-Methyl-3-nitrothieno[2,3-*g*]quinoline-4,9-dione (**9**)

Compound **8** (229 mg, 1 mmol) was solved in con. H₂SO₄ (2 mL). After cooling to 0 °C, KNO₃ (150mg, 1.5 mol, 1.5 eq) was added in portion and the mixture was stirred at 0 °C for 1.5 h, and then was poured into water (20 mL) and neutralized with K₂CO₃ to pH 8–9. The formed precipitate was filtered off, dried, and purified by prep-HPLC to give **3** (140 mg, yield 51%) and **9** (93 mg, yield 34%) as yellow crystals. Preparative HPLC was carried out using a C18 reverse phase column (150 × 30 mm, 5μm; Boston Green ODS) with a linear gradient of 0–100% CH₃CN in 0.05% aqueous HCl over 15 min at 40 °C at a flow rate of 10.0 mL/min. The eluents were collected at RT = 9.5 min for **3** and at RT = 12.0 min for **9**. ¹H NMR (400 MHz, DMSO-*d*₆) δ: 8.99 (s, 1 H), 8.87 (d, *J* = 4.8 Hz, 1 H), 7.72 (d, *J* = 4.8 Hz, 1 H), 2.78 (s,

3 H). MS (ESI) m/z : 275.2 (M+1). ^{13}C NMR (100 MHz, DMSO- d_6) δ : 177.90, 173.65, 152.45, 150.10, 147.10, 144.70, 134.25, 131.80, 131.00, 128.15. HRMS (ESI) m/z : calcd for $\text{C}_{12}\text{H}_7\text{N}_2\text{O}_4\text{S}$ [M+H] $^+$ 275.0048, Found 275.0125. MS (ESI) m/z : 274.8 (M+H).

4.1.2. 2-Amino-8-methylthieno[2,3-*g*]quinoline-4,9-dione (**10a**)

To a stirred solution of **3** (28 mg, 0.1 mmol) in MeOH and DMF (5 mL, v/v=3/1), $\text{NiCl}_2 \cdot 6\text{H}_2\text{O}$ (47 mg, 2 eq) and NaBH_4 (8 mg, 2 eq) were added at 0°C. The resulting black suspension was stirred at 0 °C for 5 min. The reaction was quenched with saturated aqueous NH_4Cl (5 mL), diluted with H_2O (5 mL) and extracted with CH_2Cl_2 (3 \times 10 mL). The combined organic layers were washed with H_2O (5 mL), dried over Na_2SO_4 , filtered and concentrated under reduced pressure to afford the crude product, which was purified by flash column chromatography eluting with CH_2Cl_2 / MeOH (90:10) to give **10a** as a brown powder (7.5 mg, yield 32.2%). ^1H NMR (400 MHz, DMSO- d_6) δ : 8.70 (d, J = 4.80 Hz, 1H), 7.57 (d, J = 4.80 Hz, 1H), 7.55 (br s, 2H), 6.34 (s, 1H), 2.75 (s, 3H). ^{13}C NMR (100 MHz, DMSO- d_6) δ : 177.25, 176.57, 165.90, 151.14, 150.08, 148.83, 143.28, 131.75, 129.40, 127.50, 101.61, 22.36. HRMS (ESI) m/z : calcd for $\text{C}_{12}\text{H}_9\text{N}_2\text{O}_4\text{S}$ [M+H] $^+$ 245.0306, Found 245.2208. MS (ESI) m/z : 245.2 (M+H). Chemical synthesis of compound **10b** was similar to that of compound **10a**.

4.1.3. 3-Amino-8-methylthieno[2,3-*g*]quinoline-4,9-dione (**10b**)

Yellow powder (5.5 mg, yield 20.2%). ^1H NMR (400 MHz, DMSO- d_6) δ : 8.84 (d, J = 4.40 Hz, 1H), 7.72 (d, J = 4.40 Hz, 1H), 6.93 (s, 1H), 2.81 (s, 3H). ^{13}C NMR (100 MHz, DMSO- d_6) δ : 178.82, 177.76, 162.11, 151.85, 149.86, 148.40, 143.63, 131.34,

129.06, 127.70, 109.91, 17.17. HRMS (ESI) m/z : calcd for $C_{12}H_9N_2O_4S$ $[M+H]^+$ 245.0306, Found 245.2208. MS (ESI) m/z : 245.2 (M+H).

4.1.4 8-Ethyl-2-nitrothieno[2,3-*g*]quinoline-4,9-dione(**22b**)

A solution of 5-bromo-2-nitrobenzo[*b*]thiophene-4,7-dione (**20**, 0.418 g, 1.45 mmol) in absolute ethanol (10 mL) was stirred at 0 °C. A solution of (*E*)-1,1-dimethyl-2-((*E*)-pent-2-en-1-ylidene)hydrazine (**21b**, 0.366 g, 2.90 mmol) in absolute ethanol (5 mL) was added dropwise. Then, sodium bicarbonate (425 mg, 5.0 mmol) was added in one portion. Then the resulting mixture was stirred at 45 °C for 4 h. The cooled mixture was concentrated in vacuo. The crude product was purified by silica gel chromatography (hexane: EtOAc = 8: 1) to yield the compound **22b** as a green solid (0.13 g, 31.2%). 1H NMR (400 MHz, $CDCl_3$) δ : 8.96 (d, J = 5.00 Hz, 1H), 8.44 (s, 1H), 7.58 (d, J = 5.00 Hz, 1H), 3.34 (q, J = 7.36 Hz, 2H), 1.31-1.40 (m, 3H). ^{13}C NMR (100 MHz, $CDCl_3$) δ : 179.2, 176.15, 158.20, 154.60, 151.85, 150.45, 148.90, 139.30, 129.45, 128.55, 126.15, 27.60, 13.85. HRMS (ESI) m/z : calcd for $C_{13}H_9N_2O_4S$ $[M+H]^+$ 289.0205, Found 289.0282.

Chemical synthesis of compounds **22a-u** was similar to that of compound **22b**. For the synthesis of compounds **22l-p**, toluene was used as the solvent instead of absolute ethanol, and the temperature and reaction time were increased to 110 °C and 16-24 h, respectively.

4.1.5 7,8-Dimethyl-2-nitrothieno[2,3-*g*]quinoline-4,9-dione(**22a**)

Yellow solid (15 mg, yield 28.1%). 1H NMR (400 MHz, $CDCl_3$) δ : 8.82 (s, 1H), 8.43 (s, 1H), 2.83 (s, 3H), 2.50 (s, 3H). ^{13}C NMR (100 MHz, $CDCl_3$) δ : 179.5, 176.2,

157.0, 154.6, 149.5, 149.0, 148.2, 139.0, 138.8, 128.5, 125.5, 18.0, 17.5. HRMS (ESI) m/z : calcd for $C_{13}H_9N_2O_4S$ $[M+H]^+$ 289.0205, Found 289.0282. MS (ESI) m/z : 288.99 (M+H).

4.1.6. 2-Nitro-8-propylthieno[2,3-g]quinoline-4,9-dione (**22c**)

Greyish green solid (166 mg, yield 32.4%). 1H NMR (400 MHz, $CDCl_3$) δ : 8.94 (d, $J = 5.04$ Hz, 1H), 8.41-8.46 (m, 1H), 7.53 (d, $J = 4.76$ Hz, 1H), 3.22-3.31 (m, 2H), 1.68-1.75 (m, 2H), 1.09 (t, $J = 7.40$ Hz, 3H). ^{13}C NMR (100 MHz, $CDCl_3$) δ : 179.07, 176.08, 157.16, 156.43, 153.75, 150.37, 148.93, 139.40, 130.37, 128.42, 125.84, 36.58, 23.45, 14.21. HRMS (ESI) m/z : calcd for $C_{14}H_{11}N_2O_4S$ $[M+H]^+$ 303.0361, Found 303.0438. MS (ESI) m/z : 303.00 (M+H).

4.1.7. 8-Buthy-2-nitrothie[2,3-g]quinoline-4,9-dione(**22d**)

Gray solid (12 mg, yield 20.0%). 1H NMR (400 MHz, $DMSO-d_6$) δ : 8.91 (d, $J = 4.88$ Hz, 1 H), 8.50 (s, 1 H), 7.74 (d, $J = 4.88$ Hz, 1 H), 3.19-3.24 (m, 2 H), 1.59 (q, $J = 7.56$ Hz, 2 H), 1.43 (t, $J = 7.34$ Hz, 2 H), 0.95 (t, $J = 7.28$ Hz, 3 H). ^{13}C NMR (100 MHz, $CDCl_3$) δ : 178.99, 176.01, 157.04, 156.81, 153.67, 150.25, 148.92, 139.34, 130.38, 128.34, 125.81, 34.43, 32.27, 22.88, 13.83. HRMS (ESI) m/z : calcd for $C_{15}H_{13}N_2O_4S$ $[M+H]^+$ 317.0518, Found 317.2461.

4.1.8. 7-Methyl-2-nitrothien[2,3-g]quinoline-4,9-dione(**22e**)

Yellow solid (40 mg, yield 32.4%). 1H NMR (400 MHz, $CDCl_3$) δ : 8.95 (s, 1H), 8.48 (s, 1H), 8.37 (s, 1H), 2.60 (s, 3H). ^{13}C NMR (100 MHz, $CDCl_3$) δ : 176.95, 175.57, 155.52, 146.05, 145.98, 140.43, 138.80, 137.92, 134.49, 129.69, 125.74, 18.45. HRMS (ESI) m/z : calcd for $C_{12}H_7N_2O_4S$ $[M+H]^+$ 275.0048, Found 275.0125.

MS (ESI) m/z : 274.96 (M+H).

4.1.9. 7-Ethyl-2-nitrothieno[2,3-g]quinoline-4,9-dione (22g)

Brown solid (32 mg, yield 65.2%). ^1H NMR (400 MHz, CDCl_3) δ : 8.96 (s, 1H), 8.49 (s, 1H), 8.39 (s, 1H), 2.90 (q, $J = 7.52$ Hz, 2H), 1.39 (t, $J = 7.64$ Hz, 3H). ^{13}C NMR (100 MHz, CDCl_3) δ : 177.47, 176.05, 157.38, 155.41, 146.63, 146.60, 145.13, 140.92, 133.77, 130.38, 126.21, 26.32, 14.59. HRMS (ESI) m/z : calcd for $\text{C}_{13}\text{H}_9\text{N}_2\text{O}_4\text{S}$ $[\text{M}+\text{H}]^+$ 289.0205, Found 289.0282.

4.1.10. 2-Nitro-7-propylthieno[2,3-g]quinoline-4,9-dione (22h)

Gray solid (23 mg, yield 50.5%). ^1H NMR (400 MHz, CD_3OD) δ : 8.90 (s, 1H), 8.51 (s, 1H), 8.48 (s, 1H), 2.89 (t, $J = 7.60$ Hz, 2H), 1.77-1.83 (m, 2H), 1.04 (t, $J = 7.2$ Hz, 3H). ^{13}C NMR (100 MHz, CD_3OD) δ : 171.28, 169.01, 154.40, 151.76, 147.98, 146.94, 146.54, 144.04, 134.23, 128.65, 125.62, 34.44, 23.56, 12.47. HRMS (ESI) m/z : calcd for $\text{C}_{14}\text{H}_{11}\text{N}_2\text{O}_4\text{S}$ $[\text{M}+\text{H}]^+$ 303.0361, Found 303.0438.

4.1.11. 7-Butyl-2-nitrothieno[2,3-g]quinoline-4,9-dione (22i)

Gray solid (30 mg, yield 75.1%). ^1H NMR (400 MHz, CDCl_3) δ : 8.96 (s, 1H), 8.51 (s, 1H), 8.39 (s, 1H), 2.87 (t, $J = 7.60$ Hz, 2H), 1.74 (q, $J = 7.60$ Hz, 2H), 1.39-1.48 (m, 2H), 1.00 (t, $J = 7.40$ Hz, 3H). ^{13}C NMR (100 MHz, CDCl_3) δ : 176.83, 175.59, 156.45, 153.85, 146.43, 145.98, 143.79, 140.31, 133.66, 130.08, 125.10, 32.06, 31.72, 21.38, 12.21. HRMS (ESI) m/z : calcd for $\text{C}_{15}\text{H}_{13}\text{N}_2\text{O}_4\text{S}$ $[\text{M}+\text{H}]^+$ 317.0518, Found 317.2461.

4.1.12. 7-Isopropyl-2-nitrothieno[2,3-g]quinoline-4,9-dione (22j)

Deep yellow solid (20 mg, 38.1%). ^1H NMR (400 MHz, CDCl_3) δ : 9.00 (d, $J =$

2.00 Hz, 1H), 8.49 (s, 1H), 8.42 (d, $J = 2.00$ Hz, 1H), 3.21 (td, $J = 6.80, 13.9$ Hz, 1H), 1.41 (d, $J = 7.00$ Hz, 6H). ^{13}C NMR (100 MHz, CDCl_3) δ : 177.53, 176.05, 157.41, 154.68, 149.61, 146.76, 146.62, 140.93, 132.34, 130.49, 126.23, 32.16, 23.22. HRMS (ESI) m/z : calcd for $\text{C}_{14}\text{H}_{11}\text{N}_2\text{O}_4\text{S}$ $[\text{M}+\text{H}]^+$ 303.0361, Found 303.0438. MS (ESI) m/z : 302.99 (M+H).

4.1.13. 7-(Tert-Butyl)-2-nitrothieno[2,3-g]quinoline-4,9-dione (**22k**)

Gray solid (18 mg, yield 55.2%). ^1H NMR (400 MHz, CDCl_3) δ : 9.15 (d, $J = 2.00$ Hz, 1H), 8.51 (d, $J = 2.00$ Hz, 1H), 8.47 (s, 1H), 1.47 (s, 9H). ^{13}C NMR (100 MHz, CDCl_3) δ : 177.61, 176.05, 157.40, 153.54, 151.93, 146.69, 146.29, 140.94, 131.58, 130.05, 126.21, 34.66, 30.65. HRMS (ESI) m/z : calcd for $\text{C}_{15}\text{H}_{13}\text{N}_2\text{O}_4\text{S}$ $[\text{M}+\text{H}]^+$ 317.0518, Found 317.2461.

4.1.14. 2-Nitro-8-(2-nitrophenyl)thieno[2,3-g]quinoline-4,9-dione (**22m**)

Gray solid (25 mg, yield 25.0 %). ^1H NMR (400 MHz, CDCl_3) δ : 9.17 (d, $J = 4.76$ Hz, 1H), 8.49 (s, 1H), 8.39 (d, $J = 8.28$ Hz, 1H), 7.70-7.85 (m, 2H), 7.51 (d, $J = 4.76$ Hz, 1H), 7.30 (d, $J = 1.24$ Hz, 1H). ^{13}C NMR (100 MHz, CDCl_3) δ : 177.64, 175.64, 157.50, 154.60, 149.78, 149.35, 147.48, 146.66, 140.04, 134.19, 133.99, 129.87, 129.75, 128.48, 125.93, 125.02, 100.05. HRMS (ESI) m/z : calcd for $\text{C}_{17}\text{H}_8\text{N}_3\text{O}_6\text{S}$ $[\text{M}+\text{H}]^+$ 382.0056, Found 382.2004.

4.1.15. 8-(2-Methoxyphenyl)-2-nitrothieno[2,3-g]quinidine-4,9-dione (**22p**)

Yellow solid (32.7 mg, yield 41.0%). ^1H NMR (400 MHz, $\text{DMSO}-d_6$) δ : 8.98 (d, $J = 4.76$ Hz, 1H), 8.46 (s, 1H), 7.59 (d, $J = 4.76$ Hz, 1H), 7.39 (t, $J = 7.16$ Hz, 1H), 7.17 (d, $J = 6.28$ Hz, 1H), 6.97-7.08 (m, 2H), 3.57 (s, 3H). ^{13}C NMR (100 MHz,

DMSO- d_6) δ 177.2, 176.8, 157.2, 156.3, 154.2, 148.8, 148.5, 139.8, 130.3, 130.2, 128.5, 128.3, 127.0, 126.0, 121.2, 110.4, 55.2. HRMS (ESI) m/z : calcd for $C_{18}H_{11}N_2O_5S$ $[M+H]^+$ 367.0310, Found 367.2297.

4.2. Pharmacology

4.2.1. Strains, culture and agents

Strains were routinely incubated in YPD (1% yeast extract, 2% peptone and 2% dextrose) at 30 °C in a shaking incubator. All clinical strains are provided by Changhai Hospital of Shanghai, China. All compounds were dissolved in DMSO at 6.4 mg/mL as stock solutions. YPD+10 % (vol/ vol) Fetal Bovine Serum (FBS) [36], Spider medium [37], Lee's medium (pH = 6.8) [36], Synthetic Low-Ammonium Dextrose (SLAD) medium [38] and RPMI 1640 medium [39] are included as well. Fluconazole was purchased from Pfizer Inc.

4.2.2. Antifungal susceptibility testing

The test was performed as described previously with a few modifications [39]. The initial concentration of fungal suspension in RPMI 1640 was 5×10^3 CFU/mL. Different concentrations of compounds were added into the fungal suspension in 96-well plates and incubated at 35 °C for 24 h. The optical density at 600 nm was detected by the spectrophotometer to indicate the inhibitory of the growth of *C. albicans*. The MIC₈₀ value is the lowest concentration of the group which the compound inhibited the growth by 80 %. Each compound was tested in triplicate.

4.2.3. Time-kill curve assay

C. albicans grown overnight was washed with PBS and resuspended in RPMI 1640.

Then the suspension was diluted to 1×10^6 cells/mL, and treated with different concentrations of compounds. The cells grew in a shaking incubator (200 rpm) at 30 °C. CFUs were calculated at predetermined time points by plating suspension dilutions on YPD agar after 48 hours' incubation at 30 °C. The assay was performed for three times independently.

4.2.4. Scanning Electron Microscopy

C. albicans cells were inoculated on glass disks coated with poly-L-lysine hydrobromide (Sigma) and incubated statically at 37°C for 90 min for adhesion. Then removed non-adherent cells and the disks were incubated in fresh RPMI 1640 medium with compound treatment at 37°C for 24 h. Then the supernatant was removed and the biofilms were immersed in a fixative consisting of 2% (v/v) glutaraldehyde in 0.15 M sodium cacodylate buffer (pH 7.2) for 2 h. The samples were dehydrated in 30%, 50%, 70%, 90%, and 100% ethanol solution in turn, and dried for 1 h. Then they were coated with gold and observed through a SEM (ZEISS, MA10).

4.2.5. Cellular surface hydrophobicity assay

C. albicans CSH was measured as described previously with a few modification [23, 40, 41]. Briefly, the *C. albicans* biofilms treated with compounds for 24 h were removed from the plate surface to obtain a cell suspension in PBS ($OD_{600} = 1.0$). Then 1.2 ml suspension and 0.3 ml octane was mixed by vortexing for 3 min. OD_{600} of the aqueous phase was determined after the mixture staying at room temperature statically for another 3 min for phase separation. OD_{600} for the group without the

octane overlay was used as the control. Three replicates were performed for each group. Relative hydrophobicity was obtained as $[(OD_{600} \text{ of control} - OD_{600} \text{ after octane overlay}) / OD_{600} \text{ of the control}] \times 100\%$

4.2.6. *In vivo antifungal activity evaluation using a rat-vaginal model.*

A rat vaginal model was used to demonstrate the antifungal effect of compounds *in vivo*. [42] Briefly, female Oophorectomized Sprague-Dawley rats (Shanghai SLAC Laboratory Animal Center, China) were injected subcutaneously with oestradiol benzoate 0.5 mg (Hangzhou animal medicine factory, China) on day 2, 4, 6 and 8 after ovarian surgery. The intravaginal inoculation with 0.1mL of 1×10^7 CFU/mL *C. albicans* suspension was conducted on day 10, 11 and 12 after ovarian surgery. The suspension was delivered into the vaginal cavity through an inoculator. Compound 22B, 22C (dissolved in saline with 1% DMSO at 2, 4, and 8 mg/mL) and fluconazole (dissolved in saline at 2 mg/mL, served as positive control) was delivered intravaginally on day 1, 2 and 3 after inoculation. 100 μ L vaginal fluid was picked and cultured on the SDA agar containing chloramphenicol on the fourth day after inoculation. The CFU was determined then. The animal experiments were approved by the Animal Ethics Committee of the Second Military Medical University (Shanghai, China). During the study, rats were observed and recorded at least two times a day, measures were taken to ensure that the sorrow of animals were minimized.

4.2.7. *Toxicity evaluation using C. elegans worms*

C. elegans glp-4; sek-1 adult nematodes were used to assess the toxicity of

compounds [22]. Briefly, the nematodes were transferred to sterile liquid medium containing 6.25, 12.5, 25, 50 and 100 $\mu\text{g/mL}$ compounds as treatment groups or DMSO as control group. The worms were incubated at 25 $^{\circ}\text{C}$ for 2 d and observed daily.

4.2.8. Real-time RT-PCR assay

C. albicans biofilm was formed in 150 mm \times 25 mm cell culture dishes treated with 0.4 $\mu\text{g/mL}$ compounds or DMSO as the control for 1h. *C. albicans* cells were then collected and total RNA was isolated using Fungal RNA-out kit (TIANDS, China). Real-time quantitative PCR was performed with SYBR Green I (RR420A, TaKaRa Biotechnology, China) using ABI 7500 Real-Time PCR system (Applied Biosystems Co, USA). Primers are shown in Table S1. 18s rRNA was used as endogenous reference. The relative expression of each target gene was calibrated against the corresponding expression by control group (expression = 1). Triplicate independent experiments were conducted to generate a mean value [23].

Acknowledgements

This work was supported by the National Natural Science Foundation of China (Grant 21502224 to N. L., 81573283 to C. S.), Science and Technology Commission of Shanghai Municipality (Grant 17XD1404700), and the Shanghai “ShuGuang” Project (Grant 14SG33).

References

- [1] G.D. Brown, D.W. Denning, N.A. Gow, S.M. Levitz, M.G. Netea, T.C. White, Hidden killers: human fungal infections, *Sci Transl Med*, 4 (2012) 165rv113.
- [2] G.D. Brown, D.W. Denning, S.M. Levitz, Tackling human fungal infections,

Science, 336 (2012) 647.

[3] T. Roemer, D.J. Krysan, Antifungal drug development: challenges, unmet clinical needs, and new approaches, *Cold Spring Harb Perspect Med*, 4 (2014).

[4] F.C. Odds, A.J. Brown, N.A. Gow, Antifungal agents: mechanisms of action, *Trends Microbiol*, 11 (2003) 272-279.

[5] R. Calderone, N. Sun, F. Gay-Andrieu, W. Groutas, P. Weerawarna, S. Prasad, D. Alex, D. Li, Antifungal drug discovery: the process and outcomes, *Future Microbiol*, 9 (2014) 791-805.

[6] N. Liu, C. Wang, H. Su, W. Zhang, C. Sheng, Strategies in the discovery of novel antifungal scaffolds, *Future Med Chem*, 8 (2016) 1435-1454.

[7] M.A. Pfaller, Antifungal drug resistance: mechanisms, epidemiology, and consequences for treatment, *Am J Med*, 125 (2012) S3-13.

[8] L.E. Cowen, D. Sanglard, S.J. Howard, P.D. Rogers, D.S. Perlin, Mechanisms of Antifungal Drug Resistance, *Cold Spring Harb Perspect Med*, 5 (2014) a019752.

[9] J.A. Paiva, J.M. Pereira, New antifungal antibiotics, *Curr Opin Infect Dis*, 26 (2013) 168-174.

[10] C. Sheng, W. Zhang, New lead structures in antifungal drug discovery, *Curr Med Chem*, 18 (2011) 733-766.

[11] R. Di Santo, Natural products as antifungal agents against clinically relevant pathogens, *Nat Prod Rep*, 27 (2010) 1084-1098.

[12] Z. Jiang, N. Liu, G. Dong, Y. Jiang, Y. Liu, X. He, Y. Huang, S. He, W. Chen, Z. Li, J. Yao, Z. Miao, W. Zhang, C. Sheng, Scaffold hopping of sampangine: discovery of potent antifungal lead compound against *Aspergillus fumigatus* and *Cryptococcus neoformans*, *Bioorg Med Chem Lett*, 24 (2014) 4090-4094.

[13] Z. Jiang, N. Liu, D. Hu, G. Dong, Z. Miao, J. Yao, H. He, Y. Jiang, W. Zhang, Y. Wang, C. Sheng, The discovery of novel antifungal scaffolds by structural simplification of the natural product sampangine, *Chem Commun (Camb)*, 51 (2015) 14648-14651.

[14] C.J. Nobile, A.D. Johnson, *Candida albicans* Biofilms and Human Disease, *Annu Rev Microbiol*, 69 (2015) 71-92.

- [15] H. Zhong, D.D. Hu, G.H. Hu, J. Su, S. Bi, Z.E. Zhang, Z. Wang, R.L. Zhang, Z. Xu, Y.Y. Jiang, Y. Wang, Activity of sanguinarine against *Candida albicans* biofilms, *Antimicrobial agents and chemotherapy*, (2017).
- [16] S. Wu, Y. Wang, N. Liu, G. Dong, C. Sheng, Tackling Fungal Resistance by Biofilm Inhibitors, *J Med Chem*, 60 (2017) 2193-2211.
- [17] G. Luo, L.P. Samaranayake, *Candida glabrata*, an emerging fungal pathogen, exhibits superior relative cell surface hydrophobicity and adhesion to denture acrylic surfaces compared with *Candida albicans*, *APMIS : acta pathologica, microbiologica, et immunologica Scandinavica*, 110 (2002) 601-610.
- [18] A. Pompilio, R. Piccolomini, C. Picciani, D. D'Antonio, V. Savini, G. Di Bonaventura, Factors associated with adherence to and biofilm formation on polystyrene by *Stenotrophomonas maltophilia*: the role of cell surface hydrophobicity and motility, *FEMS microbiology letters*, 287 (2008) 41-47.
- [19] Y.H. Samaranayake, P.C. Wu, L.P. Samaranayake, M. So, Relationship between the cell surface hydrophobicity and adherence of *Candida krusei* and *Candida albicans* to epithelial and denture acrylic surfaces, *APMIS : acta pathologica, microbiologica, et immunologica Scandinavica*, 103 (1995) 707-713.
- [20] J. Midkiff, N. Borochoff-Porte, D. White, D.I. Johnson, Small molecule inhibitors of the *Candida albicans* budded-to-hyphal transition act through multiple signaling pathways, *PloS one*, 6 (2011) e25395.
- [21] P.E. Sudbery, Growth of *Candida albicans* hyphae, *Nature reviews. Microbiology*, 9 (2011) 737-748.
- [22] L.X. Zhao, D.D. Li, D.D. Hu, G.H. Hu, L. Yan, Y. Wang, Y.Y. Jiang, Effect of tetrandrine against *Candida albicans* biofilms, *PloS one*, 8 (2013) e79671.
- [23] D.D. Li, L.X. Zhao, E. Mylonakis, G.H. Hu, Y. Zou, T.K. Huang, L. Yan, Y. Wang, Y.Y. Jiang, In vitro and in vivo activities of pterostilbene against *Candida albicans* biofilms, *Antimicrobial agents and chemotherapy*, 58 (2014) 2344-2355.
- [24] C.E. Birse, M.Y. Irwin, W.A. Fonzi, P.S. Sypherd, Cloning and characterization of ECE1, a gene expressed in association with cell elongation of the dimorphic pathogen *Candida albicans*, *Infection and immunity*, 61 (1993) 3648-3655.

- [25] X. Zheng, Y. Wang, Y. Wang, Hgc1, a novel hypha-specific G1 cyclin-related protein regulates *Candida albicans* hyphal morphogenesis, *The EMBO journal*, 23 (2004) 1845-1856.
- [26] W.L. Chaffin, *Candida albicans* cell wall proteins, *Microbiology and molecular biology reviews : MMBR*, 72 (2008) 495-544.
- [27] M. Banerjee, D.S. Thompson, A. Lazzell, P.L. Carlisle, C. Pierce, C. Monteagudo, J.L. Lopez-Ribot, D. Kadosh, UME6, a novel filament-specific regulator of *Candida albicans* hyphal extension and virulence, *Molecular biology of the cell*, 19 (2008) 1354-1365.
- [28] G. Tronchin, M. Pihet, L.M. Lopes-Bezerra, J.P. Bouchara, Adherence mechanisms in human pathogenic fungi, *Medical mycology*, 46 (2008) 749-772.
- [29] F. Li, S.P. Palecek, Distinct domains of the *Candida albicans* adhesin Eap1p mediate cell-cell and cell-substrate interactions, *Microbiology*, 154 (2008) 1193-1203.
- [30] C.R. Rocha, K. Schroppel, D. Harcus, A. Marcil, D. Dignard, B.N. Taylor, D.Y. Thomas, M. Whiteway, E. Leberer, Signaling through adenylyl cyclase is essential for hyphal growth and virulence in the pathogenic fungus *Candida albicans*, *Molecular biology of the cell*, 12 (2001) 3631-3643.
- [31] V.R. Stoldt, A. Sonneborn, C.E. Leuker, J.F. Ernst, Efg1p, an essential regulator of morphogenesis of the human pathogen *Candida albicans*, is a member of a conserved class of bHLH proteins regulating morphogenetic processes in fungi, *The EMBO journal*, 16 (1997) 1982-1991.
- [32] C. Csank, K. Schroppel, E. Leberer, D. Harcus, O. Mohamed, S. Meloche, D.Y. Thomas, M. Whiteway, Roles of the *Candida albicans* mitogen-activated protein kinase homolog, Cek1p, in hyphal development and systemic candidiasis, *Infection and immunity*, 66 (1998) 2713-2721.
- [33] H. Liu, J. Kohler, G.R. Fink, Suppression of hyphal formation in *Candida albicans* by mutation of a STE12 homolog, *Science*, 266 (1994) 1723-1726.
- [34] J.D. Sobel, S. Faro, R.W. Force, B. Foxman, W.J. Ledger, P.R. Nyirjesy, B.D. Reed, P.R. Summers, Vulvovaginal candidiasis: epidemiologic, diagnostic, and therapeutic considerations, *Am J Obstet Gynecol*, 178 (1998) 203-211.

- [35] A. Fazly, C. Jain, A.C. Dehner, L. Issi, E.A. Lilly, A. Ali, H. Cao, P.L. Fidel, Jr., R.P. Rao, P.D. Kaufman, Chemical screening identifies filastatin, a small molecule inhibitor of *Candida albicans* adhesion, morphogenesis, and pathogenesis, *Proc Natl Acad Sci U S A*, 110 (2013) 13594-13599.
- [36] K.L. Lee, H.R. Buckley, C.C. Campbell, An amino acid liquid synthetic medium for the development of mycelial and yeast forms of *Candida Albicans*, *Sabouraudia*, 13 (1975) 148-153.
- [37] M.M. Maidan, L. De Rop, J. Serneels, S. Exler, S. Rupp, H. Tournu, J.M. Thevelein, P. Van Dijck, The G protein-coupled receptor Gpr1 and the Galpha protein Gpa2 act through the cAMP-protein kinase A pathway to induce morphogenesis in *Candida albicans*, *Molecular biology of the cell*, 16 (2005) 1971-1986.
- [38] C.J. Gimeno, P.O. Ljungdahl, C.A. Styles, G.R. Fink, Unipolar cell divisions in the yeast *S. cerevisiae* lead to filamentous growth: regulation by starvation and RAS, *Cell*, 68 (1992) 1077-1090.
- [39] C.a.L.S. Institute, Reference method for broth dilution antifungal susceptibility testing of yeasts-Third Edition: Approved standard M27-A3, in, CLSI, Wayne, PA, USA, 2008.
- [40] C.C. Uribe, F. Dos Santos de Oliveira, B. Grossmann, N.A. Kretzmann, T. Reverbel da Silveira, R. Giugliani, U. Matte, Cytotoxic effect of amphotericin B in a myofibroblast cell line, *Toxicol In Vitro*, 27 (2013) 2105-2109.
- [41] M. Rosenberg, Microbial adhesion to hydrocarbons: twenty-five years of doing MATH, *FEMS microbiology letters*, 262 (2006) 129-134.
- [42] F. Mondello, F. De Bernardis, A. Girolamo, A. Cassone, G. Salvatore, In vivo activity of terpinen-4-ol, the main bioactive component of *Melaleuca alternifolia* Cheel (tea tree) oil against azole-susceptible and -resistant human pathogenic *Candida* species, *BMC Infect Dis*, 6 (2006) 158.

Figure Captions

Fig. 1. Scaffold hopping and structural simplification of antifungal natural product sampangine.

Fig. 2. Summary of SAR of thieno[2,3-*g*]quinoline-4,9-dione antifungal scaffold.

Fig. 3. Compounds 22b and 22c exhibit fungicidal activity. (A and B) Time-kill curve of different concentrations of compounds **22b** and **22c** on standard *C. albicans* strain SC5314.

Fig. 4. The anti-biofilm activity of different concentrations of compounds 22b and 22c on *C. albicans* biofilms. The results were presented as a percentage compared to the control group without drug treatment. Biofilm formation results represent the mean \pm standard deviation from five independent experiments. ** $P < 0.01$ compared with the treatment-free control group, *** $P < 0.001$.

Fig. 5. Effects of compounds 22b and 22c on *C. albicans* biofilm formation. The SEM image indicated the anti-biofilm activity of different concentrations of compound 22b (A) and 22c (B). Images in the dashed boxes are zoomed and shown on the right.

Fig. 6. Compounds 22b and 22c reduced the CSH of *C. albicans*. CSH results represent the mean \pm standard deviation from three independent experiments. * $P < 0.05$ compared with the treatment-free control group, ** $P < 0.01$, *** $P < 0.001$.

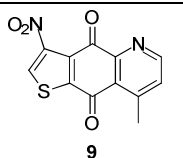
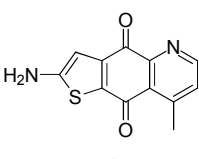
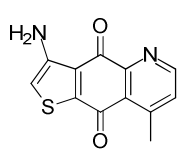
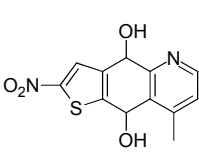
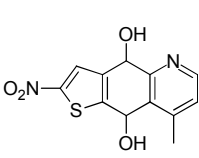
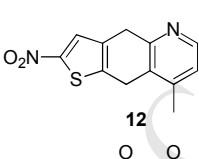
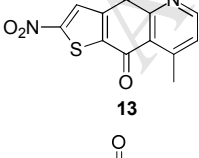
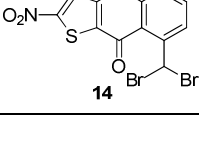
Fig. 7. Effect of different concentrations of compound 22b and 22c on the yeast-to-hypha morphological transition of *C. albicans* in YPD containing FBS medium. The cellular morphology was photographed after incubation at 37°C for 3 h.

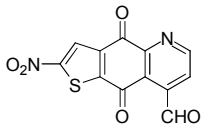
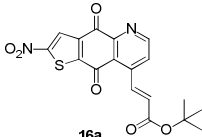
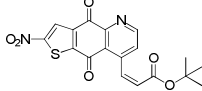
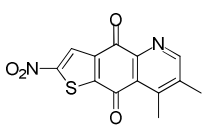
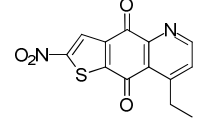
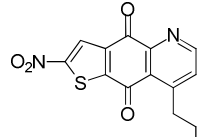
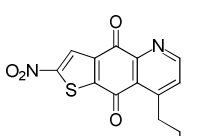
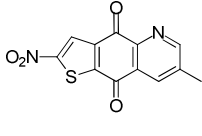
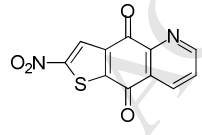
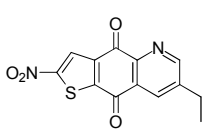
Fig. 8. Gene expression changes of some important biofilm formation related genes. The concentration of compounds **22b** and **22c** was 0.4 $\mu\text{g mL}^{-1}$. Gene expression was

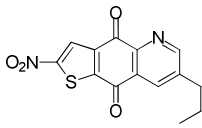
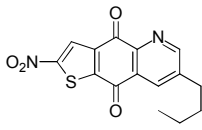
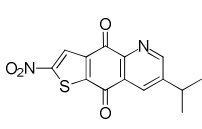
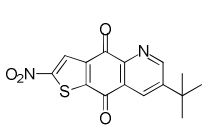
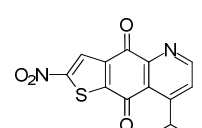
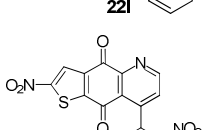
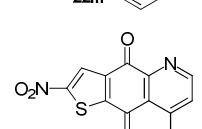
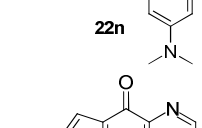
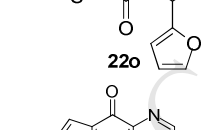
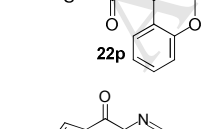
indicated as a fold change relative to that of the control group (*C. albicans* SC5314 without drug treatment). 18S rRNA was used to normalize the expression data. The data shown are mean \pm standard deviation from three independent experiments.

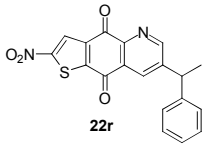
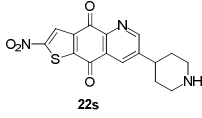
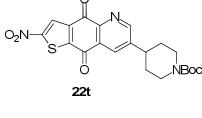
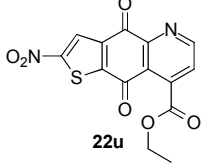
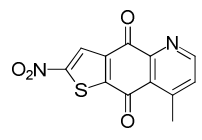
Fig. 9. Compounds 22b and 22c exhibit *in vivo* anti-fungal activity and low toxicity. (A) Compounds **22b** and **22c** are effective to treat vaginal infection of rats. (B) Compounds **22b** and **22c** show no toxicity to *C. elegans* nematodes. *C. elegans* nematodes were pipetted into medium containing different concentrations of compounds and observed daily. On day 2, the worms were photographed.

Table 1 *In vitro* antifungal activity of the simplified sampangine derivatives
(MIC₈₀, µg/mL, 24 h)^a

Compounds	<i>C. alb.</i>	<i>C. par.</i>	<i>C. gla.</i>	<i>C. neo.</i>	<i>A. fum.</i>	<i>T. rub</i>	<i>M. gyp</i>
	SC5314	22019	537	32609	07544	Cmccftla	Cmccfmza
 9	4	>64	4	4	>64	4	8
 10a	>64	>64	>64	>64	>64	8	>64
 10b	32	>64	>64	>64	>64	>64	>64
 11a (trans)	>64	>64	>64	>64	>64	>64	>64
 11b (cis)	2	8	2	4	16	2	8
 12	>64	>64	16	>64	>64	4	>64
 13	8	32	64	4	>64	8	4
 14	32	32	16	32	64	32	16

	4	8	0.125	8	16	1	2
15							
	16	32	>64	4	32	8	4
16a							
	32	>64	>64	4	>64	4	4
16b							
	0.25	0.5	1	0.25	1	0.5	1
22a							
	0.5	1	2	1	4	0.5	2
22b							
	0.5	0.5	2	1	4	2	2
22c							
	1	1	4	0.5	64	4	2
22d							
	0.5	1	1	0.5	2	1	0.5
22e							
	0.5	2	1	0.5	1	0.5	0.5
22f							
	0.5	1	1	0.25	2	0.5	0.25
22g							

	2	4	4	0.5	4	1	1
22h							
	2	4	4	0.5	4	1	1
22i							
	2	4	4	0.5	4	1	1
22j							
	2	4	4	1	4	1	1
22k							
	8	8	16	4	32	8	4
22l							
	16	>64	>64	4	64	16	8
22m							
	32	32	>64	16	>64	4	16
22n							
	4	4	4	2	16	16	8
22o							
	16	16	>64	8	16	16	16
22p							
	>64	>64	>64	0.25	32	1	1
22q							

 22r	4	4	8	0.5	4	1	1
 22s	>64	>64	>64	32	>64	>64	64
 22t	32	>64	>64	8	>64	8	16
 22u	2	4	4	4	8	1	4
 3 (ZG-20-07)	0.25	1	1	0.5	2	0.5	2
Sampangine	0.5	4	0.125	2	16	16	>64
Itraconazole	8	8	1	4	8	4	4
Fluconazole	0.25	2	2	1	>64	4	32

^a Abbreviations: *C. alb.* *Candida albicans*; *C. par.* *Candida parapsilosis*; *C. neo.* *C. glabrata*; *Cryptococcus neoformans*; *A. fum.* *Aspergillus fumigatus*; *T. rub.* *Trichophyton rubrum*; *M. gyp.* *Microsporium gypseum*.

Table 2. *In vitro* antifungal activity of the benzoquinone containing scaffolds (MIC₈₀, µg/mL, 24 h)

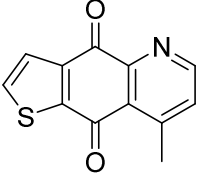
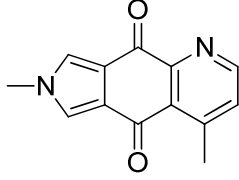
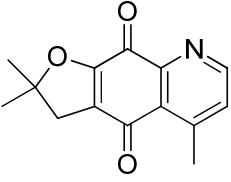
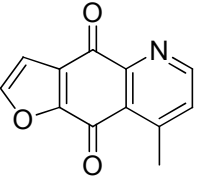
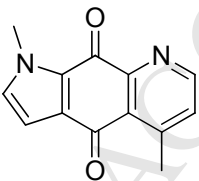
Compounds	<i>C. alb.</i>	<i>C. par.</i>	<i>C. gla.</i>	<i>C. neo.</i>	<i>A. fum.</i>	<i>T. rub</i>	<i>M. gyp</i>
	SC5314	22019	537	32609	07544	Cmccftla	Cmccfmza
 8	16	>64	8	16	16	4	>64
 23	>64	>64	>64	>64	>64	64	>64
 24	>64	>64	16	>64	64	64	>64
 25	>64	>64	>64	64	>64	>64	>64
 26	>64	>64	>64	>64	>64	>64	>64

Table 3 *In vitro* antifungal activity of compounds 22b and 22c against clinically resistant *C. albicans* strains. (MIC₈₀, µg/mL)

Compounds	Strain				
	032	1010	J38	Chang7	103
22b	0.5	0.25	0.25	0.25	0.25
22c	1	0.5	1	1	0.5
Fluconazole	>64	>64	>64	2	>64

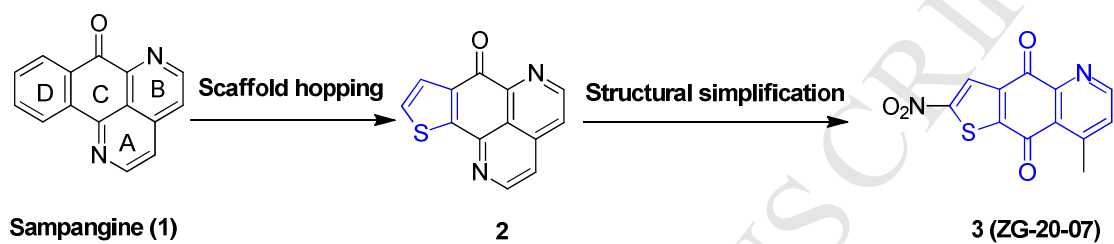


Fig. 1. Scaffold hopping and structural simplification of antifungal natural product sampangine.

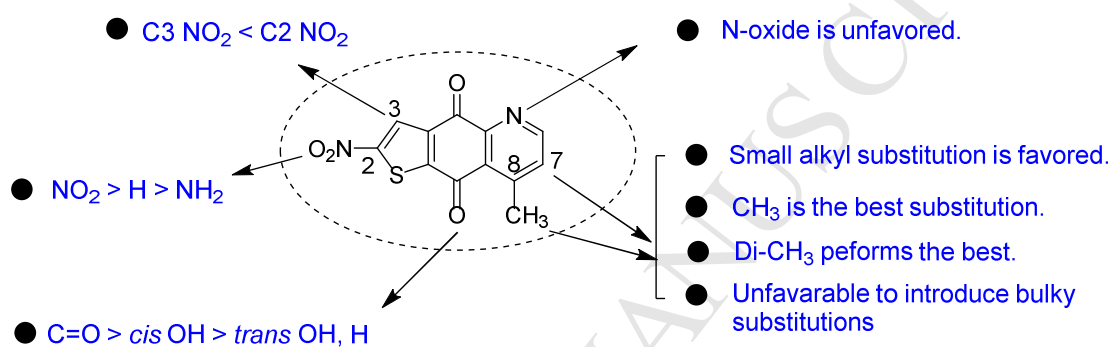


Fig. 2. Summary of SAR of thieno[2,3-g]quinoline-4,9-dione antifungal scaffold.

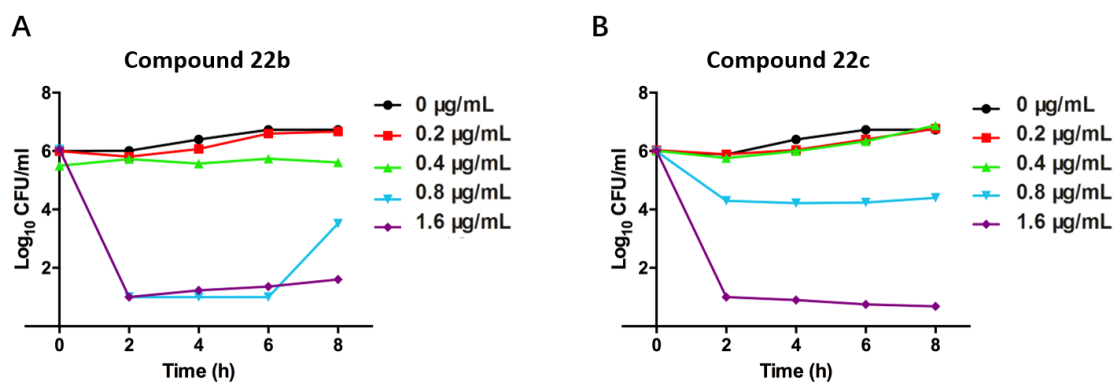


Fig. 3. Compounds 22b and 22c exhibit fungicidal activity. (A and B) Time-kill curve of different concentrations of compounds **22b** and **22c** on standard *C. albicans* strain SC5314.

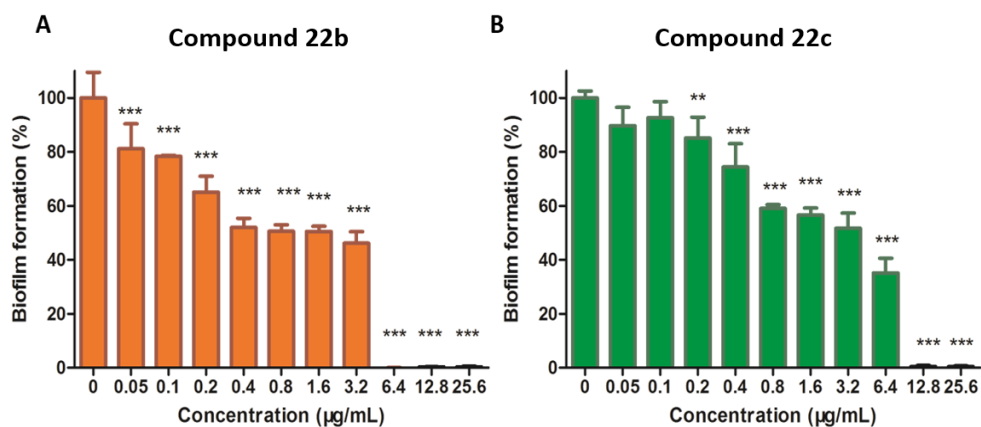


Fig. 4. The anti-biofilm activity of different concentrations of compounds 22b and 22c on *C. albicans* biofilms. The results were presented as a percentage compared to the control group without drug treatment. Biofilm formation results represent the mean \pm standard deviation from five independent experiments. ** $P < 0.01$ compared with the treatment-free control group, *** $P < 0.001$.

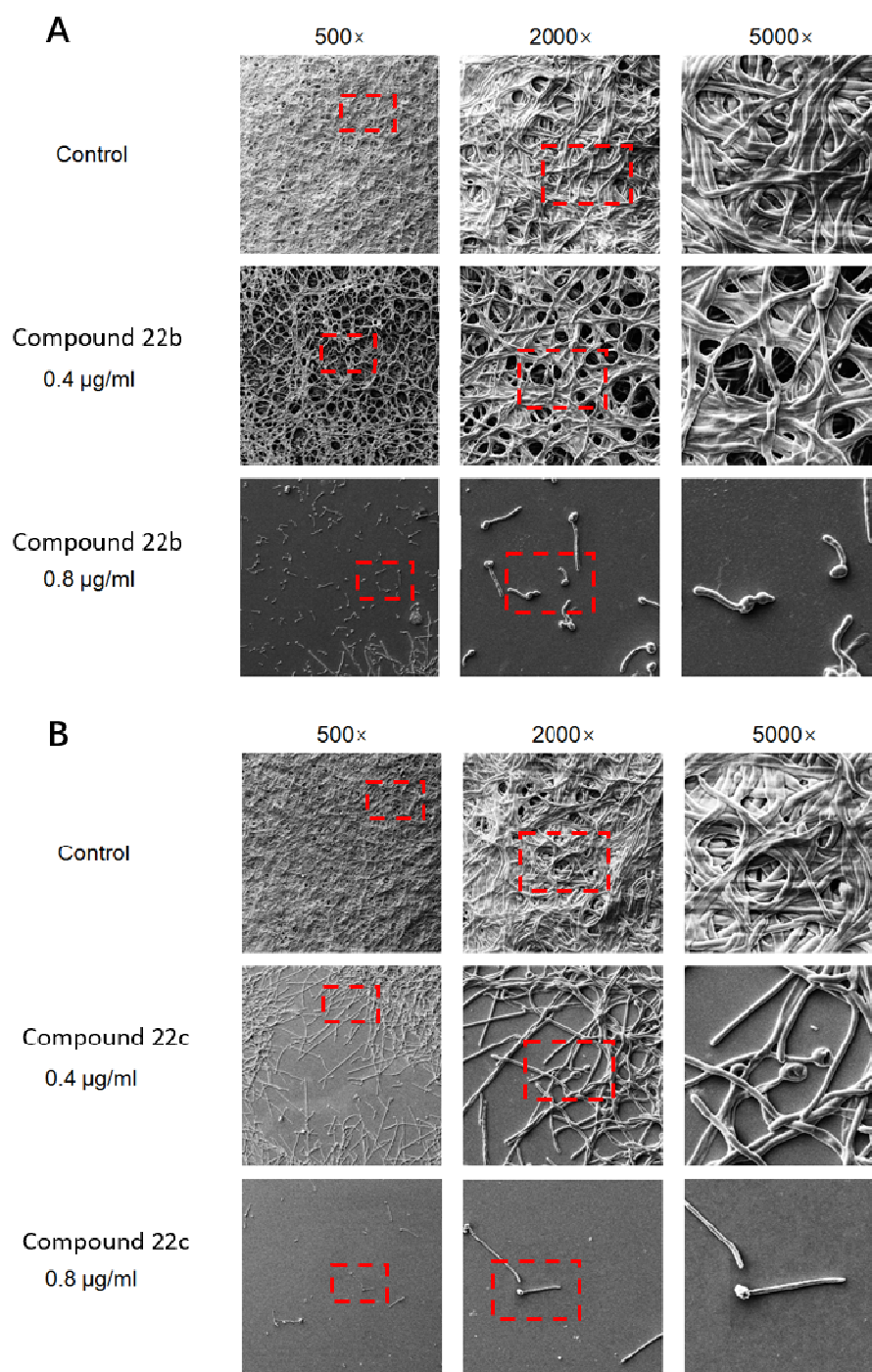


Fig. 5. Effects of compounds 22b and 22c on *C. albicans* biofilm formation. The SEM image indicated the anti-biofilm activity of different concentrations of compound 22b (A) and 22c (B). Images in the dashed boxes are zoomed and shown on the right.

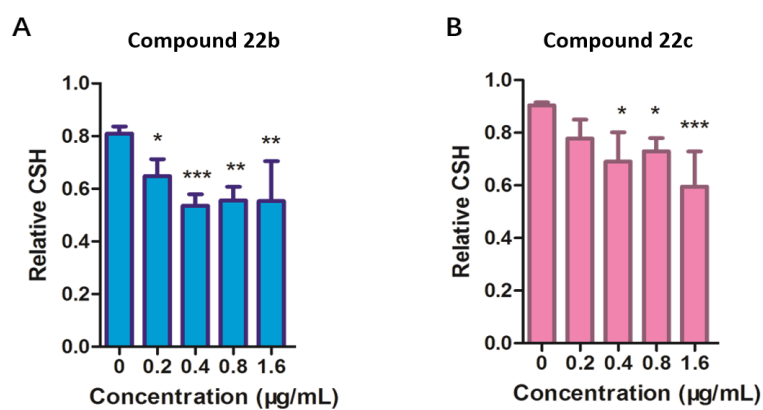


Fig. 6. Compounds 22b and 22c reduced the CSH of *C. albicans*. CSH results represent the mean \pm standard deviation from three independent experiments. * $P < 0.05$ compared with the treatment-free control group, ** $P < 0.01$, *** $P < 0.001$.

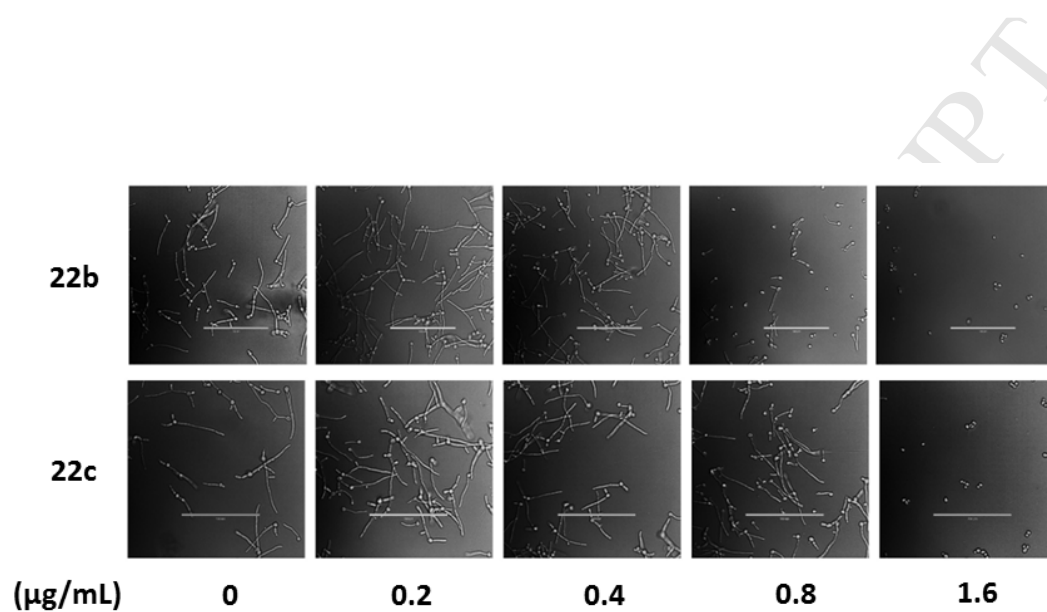


Fig. 7. Effect of different concentrations of compound 22b and 22c on the yeast-to-hypha morphological transition of *C. albicans* in YPD containing FBS medium. The cellular morphology was photographed after incubation at 37°C for 3 h.

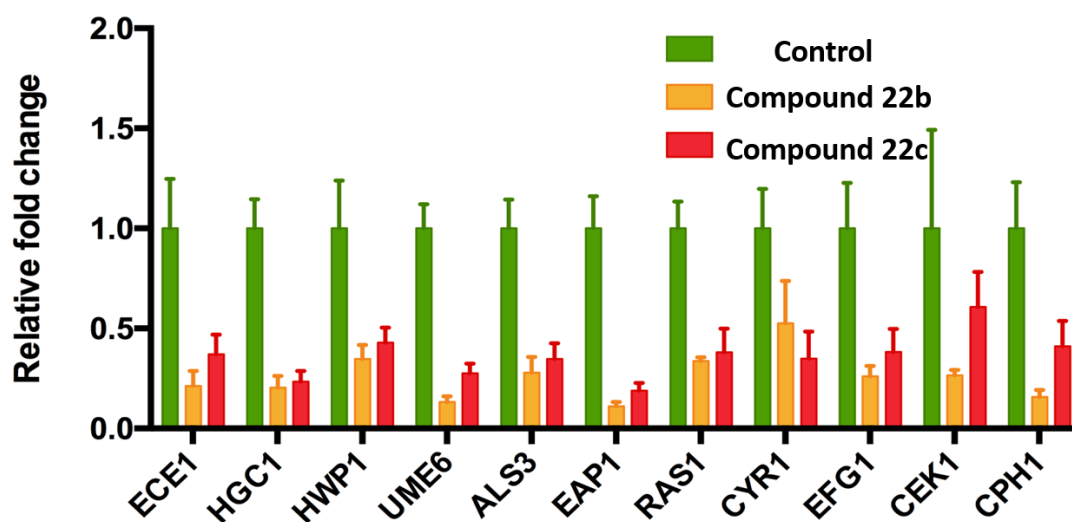


Fig. 8. Gene expression changes of some important biofilm formation related genes. The concentration of compounds 22b and 22c was $0.4 \mu\text{g mL}^{-1}$. Gene expression was indicated as a fold change relative to that of the control group (*C. albicans* SC5314 without drug treatment). 18S rRNA was used to normalize the expression data. The data shown are mean \pm standard deviation from three independent experiments.

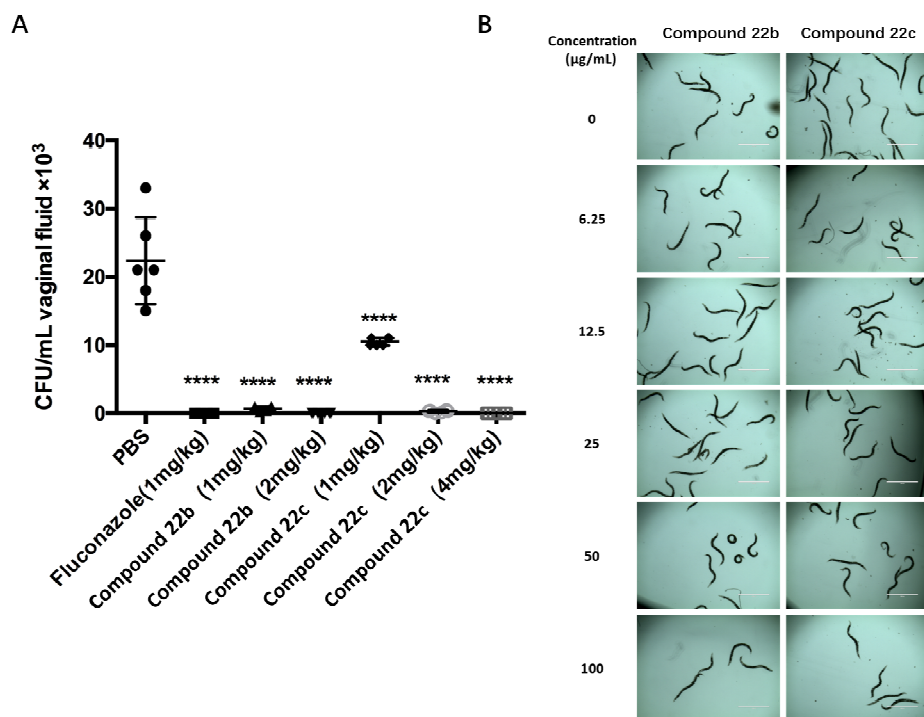
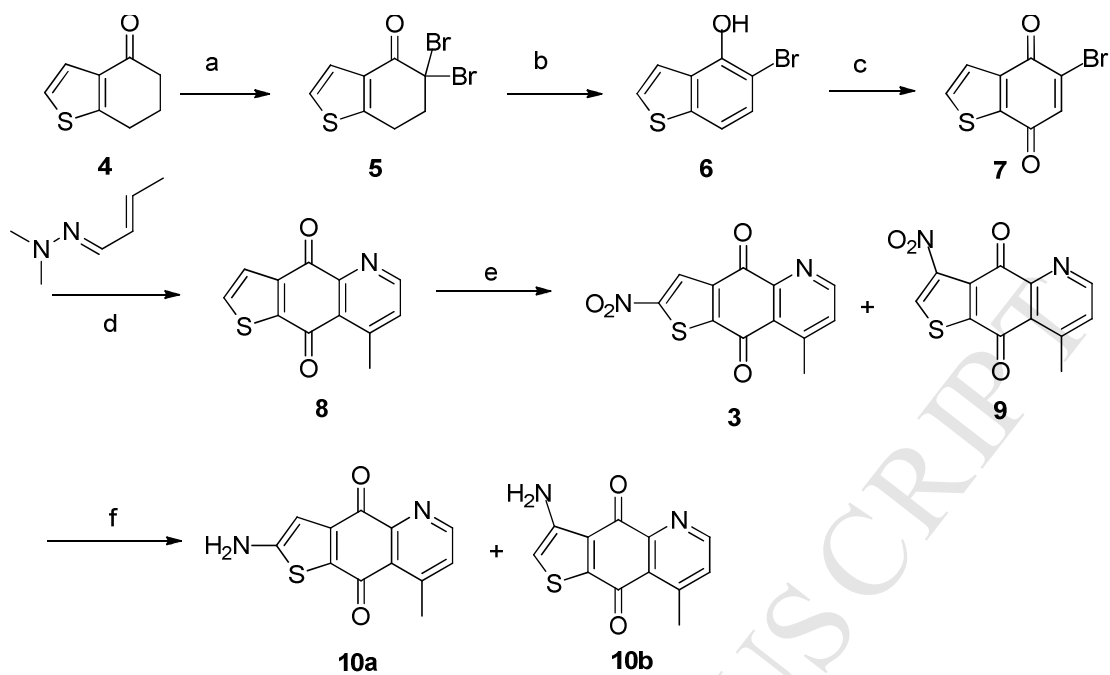
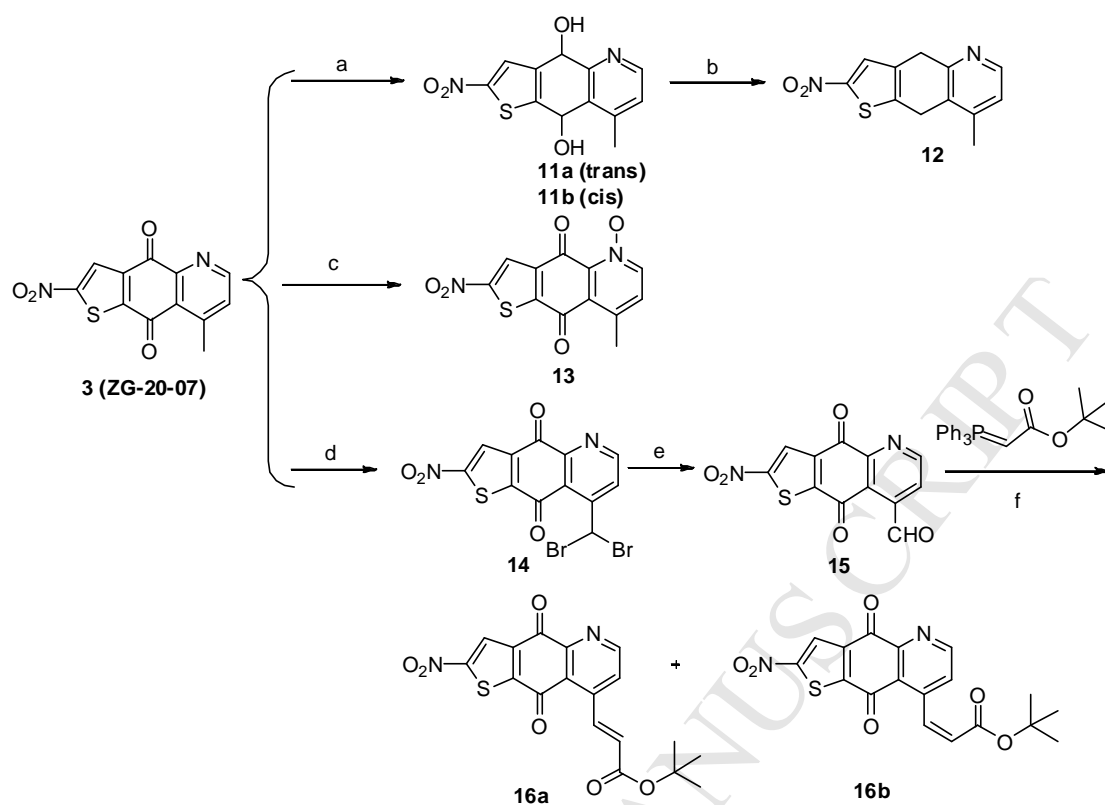


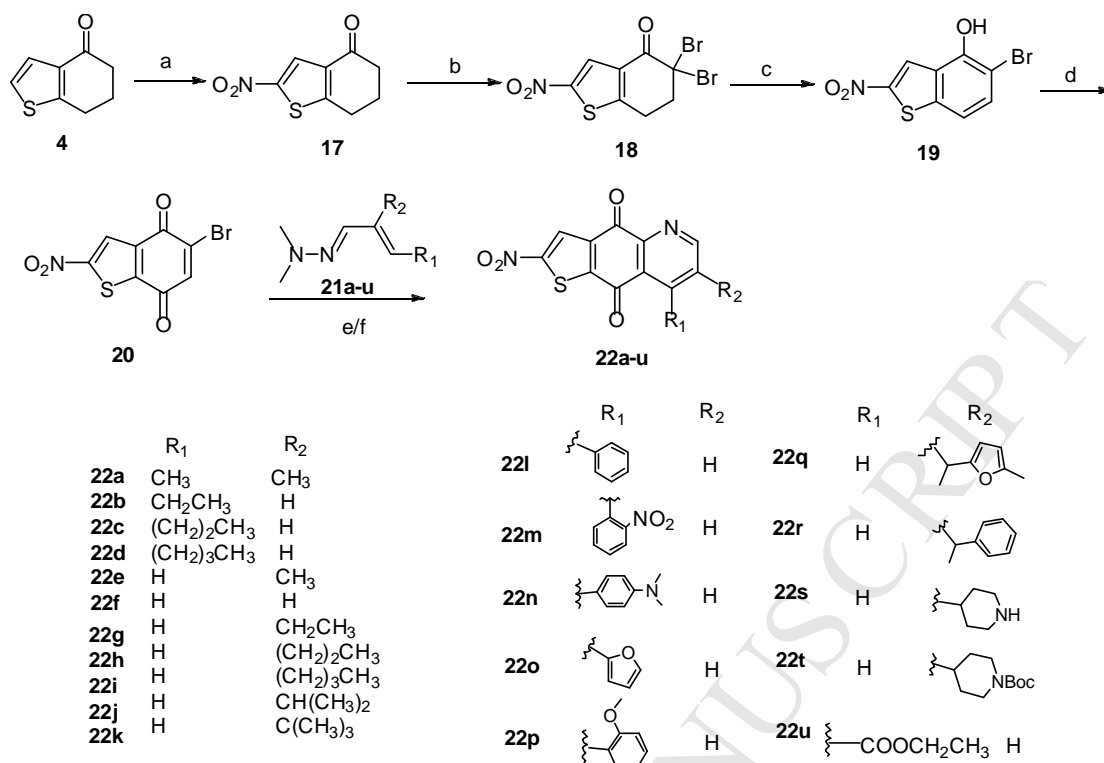
Fig. 9. Compounds 22b and 22c exhibit *in vivo* anti-fungal activity and low toxicity. (A) Compounds **22b** and **22c** are effective to treat vaginal infection of rats. (B) Compounds **22b** and **22c** show no toxicity to *C. elegans* nematodes. *C. elegans* nematodes were pipetted into medium containing different concentrations of compounds and observed daily. On day 2, the worms were photographed.



Scheme 1. Reagents and conditions: (a) $\text{CuBr}_2/\text{EtOAc}/\text{CHCl}_3$, $80\text{ }^\circ\text{C}$, 12h, 97.0%; (b) Li_2CO_3 , DMF, $100\text{ }^\circ\text{C}$, 6h, 95.8%; (c) $\text{PhI}(\text{OAc})_2$, HOAc/TFA, $0\text{-}25\text{ }^\circ\text{C}$, 0.5h, 80.5%; (d) NaHCO_3 , EtOH, 4h, $80\text{ }^\circ\text{C}$, 3h, 73.1%; (e) KNO_3 , H_2SO_4 , $0\text{ }^\circ\text{C}$, 2h, 85.0%; (f) NaBH_4 , NiCl_2 , MeOH/DMF (v/v=1/3, $0\text{ }^\circ\text{C}$, 10 min, 20.2-32.2%.



Scheme 2. Reagents and conditions: (a) NaBH_4 , DMF, 25 °C, 30 min, 19.5-27.5%; (b) HCl, DMF, 40 °C, 2 h, 70.0%; (c) $(\text{CF}_3\text{CO})_2\text{O}/\text{H}_2\text{O}_2/\text{CH}_3\text{CO}_2\text{H}$ /-10 °C, 12 h, 55.2%; (d) Br_2 , HOAc, 110 °C, 3 h, 82.5%; (e) DMSO, 120 °C, 4 h, 90.4%; (f) THF, 25 °C, 12 h, 31.2-32.3%.



Scheme 3. Reagents and conditions: (a) KNO₃, H₂SO₄, 0 °C, 1 h, 90.2%; (b) CuBr₂/EtOAc/CHCl₃, 80 °C, 12 h, 92.0%; (c) Li₂CO₃, DMF, 100 °C, 6 h, 96.0%; (d) PhI(OAc)₂, HOAc/TFA, 0-25 °C, 0.5 h, 85.3%; (e) EtOH, NaHCO₃, 45 °C, 4-12h, 13.0-75.1%; (f) NaHCO₃, toluene, 110°C, 16-24 h, 25.0-41.0%; (g) 4 N HCl/MeOH, 55 °C, 12 h, 90.0%; (h) HATU, Et₃N, DMF, 30 °C, 2-12 h, 11.9-84.2%.

Research Highlights

- Novel simplified analogues of antifungal natural product sampangine were designed, synthesized and evaluated.
- Compounds **22b** and **22c** showed good fungicidal activity against both fluconazole-sensitive and fluconazole-resistant *Candida albicans* strains.
- Compounds **22b** and **22c** were proven to be novel *Candida albicans* biofilm inhibitors.
- Compounds **22b** and **22c** showed excellent *in vivo* antifungal potency with low toxicity.